HHS Public Access

Author manuscript

Am J Transplant. Author manuscript; available in PMC 2024 April 01.

Published in final edited form as:

Am J Transplant. 2023 October ; 23(10): 1526–1535. doi:10.1016/j.ajt.2023.06.011.

Microbiota-dependent and -independent effects of obesity on transplant rejection and hyperglycemia

Zhipeng Li[*,1,2], **Luqiu Chen**[*,1], **Martin Sepulveda**[1], **Peter Wang**[1], **Mladen Rasic**[3], **Stefan G. Tullius**[4], **David Perkins**[3,5], **Maria-Luisa Alegre, MD, PhD**[1]

[1]Department of Medicine, University of Chicago, Chicago, IL

[2]Current address: College of Food Science & Technology, Nanchang University, Nanchang 330047, PR China

[3]Department of Nephrology, University of Illinois at Chicago, Chicago, IL

[4]Division of Transplant Surgery, Department of Surgery, Brigham and Women's Hospital, Harvard Medical School, Boston, MA

[5]Current address: Department of Medicine, University of New Mexico, Albuquerque, NM

Abstract

Obesity is associated with dysbiosis and a state of chronic inflammation that contributes to the pathogenesis of metabolic diseases, including diabetes. We have previously shown that obese mice develop glucose intolerance, increased alloreactivity and accelerated transplant rejection. In the present study, we investigated the influence of the microbiota on diet-induced obesity (DIO)-associated transplant rejection and hyperglycemia. Antibiotic treatment prolonged graft survival and reduced fasting glycemia in high fat diet (HFD)-fed specific pathogen-free (SPF) mice, supporting a role for the microbiota in promoting accelerated graft rejection and hyperglycemia induced by DIO. Further supporting a microbiota-dependent effect, fecal microbiota transfer (FMT) from DIO SPF mice into germ-free (GF) mice also accelerated graft rejection when compared to lean mice-FMT. Notably, HFD could be also detrimental to the graft independently from microbiota, obesity, and hyperglycemia. Thus, whereas HFD-associated hyperglycemia was exclusively microbiota-dependent, HFD affected transplant outcomes via both microbiota-dependent and -independent mechanisms. Importantly, hyperglycemia in DIO SPF mice could be reduced by the addition of the gut commensal *Alistipes onderdonkii*, which alleviated both HFD-induced inflammation and glucose intolerance. Thus, microbial dysbiosis can be manipulated via antibiotics or select probiotics to counter some of the pathogenic effects of obesity in transplantation.

Keywords

organ transplantation; obesity; gut microbiota; inflammation; diabetes

Correspondence to: Maria-Luisa Alegre, MD, PhD, 924 E. 57th St., JFK-R314, Chicago, IL 60637.

*Co-first authors

The authors declare no conflict of interest pertinent to this study.

Introduction

Pre-existing risk factors such as dietary habits and obesity contribute to diabetes not only in the general population but even more so in transplant recipients who are more susceptible to developing diabetes (1). In solid organ transplantation, accumulating evidence has shown that obesity, a chronic low-level inflammatory state, contributes to shortened transplant survival and is associated with increased risk of postoperative complications (2). Moreover, the use of immunosuppressants contributes to the pathogenesis of post-transplantation diabetes mellitus (PTDM). For example, corticosteroids can promote gluconeogenesis, disturb insulin signaling and cause hyperglycemia (3, 4) and tacrolimus can impair pancreatic β-cell function and lead to PTDM (5).

We have previously shown that mice on a high-fat diet (HFD) develop hyperglycemia and reject allografts faster than mice on a low-fat diet (LFD) (6–8). HFD induces systemic inflammation, which may contribute to both the acceleration of transplant rejection (9) and the development of insulin resistance (10). In parallel, we and others have shown that the microbiome influences both transplant outcomes (11–14) and diabetes susceptibility (15). Given that diet determines the membership composition of the microbiota, it is conceivable that some of the effects of HFD on transplant rejection kinetics are microbiota dependent. For instance, we have reported that a diet rich in fat and sugar increases the abundance of *Oscillibacter valericigenes*, which increases the numbers of $Mmp12^{+}$ macrophages in adipose tissue, thus leading to insulin resistance (16).

In the present study, we aimed to investigate whether the microbiota has a causal role on the capacity of HFD to accelerate allograft rejection and induce hyperglycemia. Our results show that HFD accelerated transplant rejection through both microbiota-dependent and -independent mechanisms. HFD-induced hyperglycemia on the other hand was driven only by the microbiota as it failed to occur in HFD-fed GF mice. While the HFD-induced dysbiosis enabled hyperglycemia, we also identified a gut microbial community member, *Alistipes onderdonkii*, that improved both HFD-induced inflammation and HFD-induced glucose intolerance when supplemented to SPF mice, in the absence of reduced body weight. Our results indicate that both diet alone, and the interaction between diet and microbiota play an important role in regulating alloimmune responses and graft outcome, offering insights for novel solutions in the setting of PTDM.

Results

HFD-induced obesity is associated with hyperglycemia and accelerated allograft rejection

Six to 8 week-old C57Bl/6 (B6, $H\text{-}2^{b}$) male mice were maintained under SPF conditions and started on either a HFD or a normal chow diet (NC). Longitudinal fecal samples were collected every 2–4 days after 7 weeks of diet prior to transplantation, and a fully mismatched DBA/2 ($H\text{-}2^{d}$) skin graft was placed after at least 8 weeks of diet (Fig. 1A). Immediately prior to transplantation, HFD-fed mice exhibited distinct and stable fecal microbiome composition, evident obesity and higher fasting blood glucose levels compared to NC-fed mice (Fig 1B–D). Confirming our previously published data, DIO mice rejected their transplants significantly faster than lean mice (Fig. 1E). Donor-specific antibody

(DSA) titers were determined from sera sampled on two occasions, immediately prior to transplantation and 20 days later. As expected, DSA levels were markedly elevated in both DIO and lean mice post-transplantation (Fig. 1F).

Antibiotic treatment improves hyperglycemia and prolongs allograft survival

To investigate the role of HFD-associated dysbiosis in accelerating transplant rejection in obese mice, DIO SPF mice were gavaged daily with a broad-spectrum antibiotic cocktail (Abx) or vehicle daily for 10 days prior to transplantation. (Fig. 2A). Abx-treatment did not reduce body weight (Fig. 2B) but resulted in significantly lower levels of fasting blood glucose (Fig. 2C). Moreover, Abx pre-treatment significantly prolonged allograft survival (Fig. 2D), suggesting a possible role for HFD-associated microbiota in hyperglycemia and accelerated graft rejection.

FMT from HFD-fed mice into GF mice results in accelerated allograft survival

As an alternative approach to investigating if the influence of HFD on transplant outcome was gut microbiota mediated, we transplanted fecal microbiota from either DIO or lean SPF mice into GF mice 12 days prior to transplantation. The recipients of FMT were started at the time of FMT on a diet matched to that of their FMT donors to support the persistence of the transferred microbiota and were maintained on their respective diets for the duration of the experiment (Fig. 3A). HFD-FMT-reconstituted hosts exhibited significantly accelerated skin graft rejection compared to NC-FMT-reconstituted host (Fig. 3B). To determine if HFD-FMT increased alloreactivity, we enumerated donor-reactive $CD4^+$ T cells in the spleen of ex-GF mice at 3 weeks post-transplantation using fluorescently labeled I-A^b tetramers loaded with a K^d-derived peptide. Consistent with their faster graft rejection, HFD-FMT-reconstituted ex-GF mice displayed increased numbers of donor-specific $CD4^+$ T cells when compared to NC-FMT-reconstituted ex-GF mice (Fig. 3C), supportive of DIO-associated microbiota's sufficiency to increase alloreactivity.

In the absence of microbiota, HFD accelerates rejection but does not impair glucose tolerance

Our previous experiments in Abx-treated DIO SPF mice and in HFD-FMT-reconstituted ex-GF mice indicated a role for HFD-associated microbiota in mediating hyperglycemia, increased alloreactivity and accelerated graft rejection. We next investigated whether some of the effects of HFD could be microbiota independent. To this end, GF B6 mice devoid of microbiota received a HFD or NC diet for 12 weeks prior to DBA/2 skin transplantation (Fig. 4A). In contrast to DIO SPF mice, sterile HFD-fed GF mice were resistant to developing obesity and diabetes (Fig. 4B–C), as previously described (17, 18). However, HFD was still able to accelerate skin graft rejection in sterile GF mice (Fig. 4D), correlating with increased activation of donor-reactive splenic T cells (Fig. 4E), as a readout of alloreactivity. These results support a microbiota-independent impact of HFD on transplant outcome, but an essential role of the microbiota in HFD-associated obesity and hyperglycemia. Moreover, they also indicate that a HFD can be detrimental to the graft independently from obesity and independently from hyperglycemia.

A. onderdonkii improves HFD-induced inflammation and glucose intolerance

Our previous results indicate that accelerated transplant rejection and diabetes following HFD were partially and fully microbiota-dependent, respectively. We and others have previously reported that transplant rejection and glucose intolerance are both dependent on TNF-mediated inflammation (19, 20). We have recently identified a gut commensal, *A. onderdonkii* DMS19147, present in slow-rejecting SPF mice (14), the administration of which was sufficient to reduce TNF production by T cells and myeloid cells at homeostasis and to prolong minor mismatched allograft survival in lean SPF mice (21). To determine if this commensal could inhibit TNF production and improve glucose tolerance in the setting of HFD and DIO, we administered *A. onderdonkii* DMS19147 3 times/week starting at the time of HFD initiation (Fig. 5A). Administration of *A. onderdonkii* DMS19147 did not reduce HFD-dependent weight gain (Fig. 5B). As expected, HFD resulted in a significant increase in TNF production by LPS-stimulated $CD11b^{-}CD11c^{+}$ cells and $CD11b^{+}$ cells (Fig. 5C, D). Similar to the effects we had shown in lean SPF mice (22), *A. onderdonkii* DMS19147 administration to DIO SPF mice significantly reduced TNF production by those cells (Fig. 5C, D). Additionally, *A. onderdonkii* DMS19147 administration was sufficient to reduce the fasting blood glucose levels associated with obesity (Fig. 5E) and significantly improved glucose tolerance (Fig. 5F, G).

Discussion

Chronic inflammation is involved in both the development of insulin resistance (23) and post-transplantation complications (2). Inflammation can be induced by microbiota-dependent and microbiota-independent mechanisms. On the one hand, intestinal dysbiosis can increase gut epithelial permeability allowing microbial components to enter the circulation and activate both innate and adaptive immune responses via microbe-associated molecular patterns, thus contributing to systemic inflammation in a microbiota-dependent process. On the other hand, dying adipocytes resulting from adipose tissue hypertrophy-mediated ischemia and hypoxia can recruit and activate macrophages via damage-associated molecular patterns, contributing to sterile inflammation (24), a microbiota-independent process.

A number of studies have demonstrated that diet shapes the composition of the gut microbiota, which further regulates immune responses and energy metabolism (25). In this work, we show that DIO promotes both the accelerated rejection of transplants and the onset of glucose intolerance. Moreover, perturbations of the gut microbiota induced by HFD in SPF mice were sufficient to significantly affect alloimmunity, transplant outcomes and blood sugar levels, indicating a causal role for the gut microbiota in regulating alloimmune responses and metabolism. In parallel, our results also identify a microbiota-independent effect of HFD in its ability to accelerate graft rejection. Thus, HFD can be detrimental to graft survival (i) independently from obesity and from diabetes, and (ii) independently from its associated dysbiotic state, as sterile GF mice fed a HFD were resistant to obesity and hyperglycemia but still developed accelerated graft rejection. Therefore, HFD can impair transplant outcomes through both microbiota-dependent and independent mechanisms, and

independently from obesity and hyperglycemia. We hypothesize that these distinct effects correspond to microbiota-based inflammation and to sterile inflammation, respectively.

There have been conflicting results regarding whether GF mice are resistant or not to diet-induced hyperglycemia. Whereas we found that our HFD did not cause obesity or hyperglycemia in GF B6 mice, another study reported that western diet induced adiposity and glucose intolerance equally in SFP and GF B6 mice (26). Conversely, Logan *et al* (27) reported that HFD significantly induced body weight gain but failed to cause glucose intolerance in GF Swiss Webster mice, though blood glucose levels were trending up. Different diets interact differently with the gut microbiota and the host, with certain HFDs containing nutrients such as fiber that require the gut microbiota for processing and optimal calorie utilization, while other HFDs lower in fiber and richer in end products are less dependent on the microbiota for digestion. Although the microbiota may not be an indispensable factor in the onset of diabetes, undoubtedly it is a contributing factor that can mediate and exacerbate the detrimental effects of HFD.

We previously identified a gut commensal, *A. onderdonkii*, whose presence in mice obtained from Jackson Laboratories (JAX) was associated with prolonged survival of minor mismatched skin grafts when compared with rejection kinetics observed in mice obtained from Taconic Farms (TAC) which lacked this intestinal bacterium (14). Cohousing of JAX and TAC mice or performing FMT from JAX to TAC mice were sufficient for transient establishment of *A. onderdonkii* in TAC mice and to convert the TAC-associated fast rejecting phenotype into a slow rejecting one (14). More recently, we showed that oral supplementation with *A. onderdonkii* DSM19147 in TAC mice was sufficient to prolong graft survival, and this correlated with reduced production of TNF by T cells and myeloid cells both at steady state and after transplantation (22). Prolonged graft survival induced by *A. onderdonkii* supplementation was similar to that in animals treated with a blocking TNF antibody and *A. onderdonkii* administration did not improve graft survival in anti-TNF-treated mice (22), suggesting that the graft-protecting effect of *A. onderdonkii* was dependent on its ability to reduce TNF production. DIO is also associated with TNF-dependent inflammation (28). In this work, we show that *A. onderdonkii* supplementation also reduced TNF production by myeloid cells in obese mice, improving HFD-induced inflammation. Consistently, *A. onderdonkii* also improved glucose tolerance. Thus, *A. onderdonkii* serves as an example gut microbe that can both slow transplant rejection and improve glucose tolerance through its anti-inflammatory properties and that can counteract select effects of obesity-associated dysbiosis.

In summary, this study shows that HFD induces systemic inflammation and exacerbates transplant rejection through both microbiota-dependent and microbiota-independent mechanisms, whereas its hyperglycemia-promoting effects rely more on diet's interaction with the gut microbiota. Importantly, our data also reveal a deleterious impact of HFD independent from obesity and hyperglycemia, which may be of importance for diet counseling of transplant patients regardless of their body mass index and diabetes status. Finally, we identify a gut commensal, *A. onderdonkii*, which holds potential to improve transplant outcomes and PTDM.

Materials and Methods

Bacterial cultures

A. onderdonkii DSM19147 was obtained from the DSMZ (Germany) and cultured in chopped meat medium (Anaerobe System, AS-811) in an anaerobic chamber at 37°C for 24h. Bacterial pellets were resuspended in PBS containing 10% glycerol and stored at −80 *°C* until use.

Mice

C57Bl/6 (B6, H-2^b) mice were obtained from Taconic Farms and maintained in a specific pathogen-free facility. All experiments were started on 6–8 week-old mice. Some B6 mice were bred in house and maintained in a germ-free facility. DBA/2 mice (H-2^d) were obtained from Charles River. SPF mice on normal chow received irradiated diet from Envigo (Harlan, Teklad-2918). For HFD experiments, SPF male B6 mice were fed irradiated diet from Research Diets Inc. (New Brunswick, NJ, D12492, 60% calories from Fat) for 8–12 weeks. For the antibiotic treatment experiment, animals were daily gavaged for 10 days prior skin transplantation with 200μL antibiotic cocktail solution containing gentamycin (0.35 mg/mL, Fresenius Kabi), kanamycin (5.25 mg/mL, Gibco, Thermo Fisher Scientific), colistin (8500 U, RPI), metronidazole (2.15 mg/mL, Sigma-Aldrich), and vancomycin (0.5 mg/mL, Hospira) diluted in autoclaved water. Some animals were simultaneously gavaged with *A. onderdonkii* DSM19147 (10^8 bacteria) or vehicle control 3 times a week starting at the initiation of the HFD and until the end of the experiment. GF mice were fed autoclaved 5K67 LabDiet for normal chow and doubly irradiated diet from Research Diets Inc. (New Brunswick, NJ, D12492-1.5V) for HFD. Animals were weighed weekly. All animal experiments were approved by the University of Chicago Animal Care and Use Committee and adhered to the standard of NIH guide for the Care and Use of Laboratory Animals.

Metagenome analyses

Fecal samples were collected from lean and obese mice longitudinally. Quality-controlled metagenomic shotgun reads were assembled de novo using Metaspades (29) with default settings. Contigs longer than 1,000 base pairs were retained for further analysis. Metagenomic binning was performed using MetaBAT2 (30) with default parameters to generate metagenome-assembled genomes (MAGs). Completeness and contamination of MAGs were assessed using CheckM v2 (31) with lineage-specific marker genes. MAGs with completeness ≥70% and contamination ≤10% were considered high-quality and used for downstream analyses. Taxonomic classification of MAGs was conducted using GTDB-Tk v2 (32) with the Genome Taxonomy Database release 207(33).

Skin transplantation

Tail skin from male DBA/2 mice was transplanted onto the flank of male SPF or GF B6 recipients as previously described (34) and bandages were removed after 7 days. Graft survival was monitored every other day thereafter. Rejection was identified by visually inspecting grafts for size, the presence of hair, pigmentation, and the development of

inflammatory spots or tissue necrosis. Rejection was determined when the graft scab fell off.

Blood glucose levels and intraperitoneal glucose tolerance test

For fasting blood glucose levels, animals were fasted overnight with free access to water and blood glucose was measured in the morning using a Freestyle Lite glucometer (Abbot Diabetes Care). For testing glucose tolerance, mice were fasted for 6 h during the light phase with free access to water. A concentration of 1.5mg/kg glucose (Sigma-Aldrich) was injected intraperitoneally. Blood glucose was measured at 0, 15, 30, 60 and 120 min post-injection.

Cell cultures and in vitro stimulation

Spleen cells were isolated, resuspended in complete DMEM (Corning) with 5–10%FBS, 1% penicillin/streptomycin, 1% L-glutamine, 1% NEAA, 1% HEPES, and 0.028 mM β-mercaptoethanol, and cultured at 37°C in 10% CO2.

Isolated spleen cells were plated in 96-well plates (2×10^6/well). Cells were stimulated with various doses of LPS (0–10ng/mL) as indicated, and brefeldin A (5μg/ml) was added into each well 60–120min after plating. After 16–20h, cells were harvested and stained for flow cytometry analyses as described below. All samples were analyzed with the LSR Fortessa (BD Biosciences).

Flow cytometry analyses

All monoclonal antibodies were purchased from BD Biosciences, Invitrogen, or eBioscience and BioLegend. Spleens were isolated from mice, homogenizedand resuspended in a signle cell suspension in DMEM. Cells were counted with a Fortessa flow cytometer prior to staining 1:1000 with fixable Live Aqua live/dead stain (Invitrogen) for 20–30 min at RT in the dark. For tetramer staining analyses, 5×10^6 unenriched spleen cells were stained with both phycoerythrin (PE) and allophycoerytherin (APC)-coupled pK^d(PEYWEEQTQRAKSD):I-A^b (NIH core facility) for 60 min at RT in a dark water bath. Cells were then surface stained with fluorophore conjugated anti-CD4 (GK1.5), anti-CD8 (53–6.7), anti-B220 (RA3-6B2), anti-CD44 (IM7) for 10 min at RT in the dark. For TNF production analyses, cells were stained with anti-CD11c (N418) and anti-CD11b (M1/70) for 10min at RT in the dark. Cells were then fixed and permeabilized with an intracellular FoxP3 staining kit (Invitrogen) according to the manufacturer's instructions and stained intracellularly with anti-FoxP3 (FJK-16s) or anti-TNF (MP6-XT22) for 30min at RT in the dark.

For DSA titer determination, serum was collected from transplant recipients and stored at −20° C. 5×10^5 DBA/2 splenocytes in PBS 2%FBS were incubated with 5μL serum for 20 min at RT. Cells were washed with PBS 2%FBS, then stained with a fixable viability dye (Invitrogen), anti-CD19 (6D5), and goat anti-mouse IgG (H+L) (catalog 1031-02, Southern Biotech) for 15 min at RT. Relative IgG was determined by the MFI of live $CD19^-$ cells. All samples were run on a LSR Fortessa 4–12, 4–15, 4–15HTS or X20 flow cytometer (BD Biosciences).

Statistical analyses

Non-parametric Mann Whitney (comparing two groups), Kruskal-Wallis followed by Dunn's multiple comparison (comparing 3 or more groups), or Logrank Mantel-Cox (for survival curves) tests were used for statistical analyses using Prism (GraphPad). Differences were considered significant at $p < 0.05$. Results are displayed as Mean +/− SEM.

Acknowledgements

This work was supported by NIH/NIAID U01 AI132898 to SGT, DP, and MLA, NIH/NIDDK TL1DK132769 to MR, and NIH/NIAID R01 AI115716 to MLA.

Abbreviations

Abx	antibiotics
APC	allophycoerytherin
C57BL/6	B6
DIO	diet-induced obesity
DSA	donor-specific antibodies
FMT	fecal microbiota transfer
GF	germ-free
HFD	high fat diet
JAX	Jackson Laboratories
LFD	low fat diet
MAG	metagenome-assembled genome
NC	normal chow
PE	phycoerythrin
PTDM	post-transplant diabetes mellitus
RT	room temperature
SPF	specific pathogen-free
TAC	Taconic Farms

References

1. Shivaswamy V, Boerner B, Larsen J. Post-Transplant Diabetes Mellitus: Causes, Treatment, and Impact on Outcomes. Endocrine reviews 2016;37(1):37–61. [PubMed: 26650437]
2. Heinbokel T, Floerchinger B, Schmiderer A, Edtinger K, Liu G, Elkhal A et al. Obesity and its impact on transplantation and alloimmunity. Transplantation 2013;96(1):10–16. doi: 10.1097/TP.1090b1013e3182869d3182862f. [PubMed: 23416683]

3. Donihi AC, Raval D, Saul M, Korytkowski MT, DeVita MA. Prevalence and predictors of corticosteroid-related hyperglycemia in hospitalized patients. Endocrine practice : official journal of the American College of Endocrinology and the American Association of Clinical Endocrinologists 2006;12(4):358–362. [PubMed: 16901792]
4. Blackburn D, Hux J, Mamdani M. Quantification of the Risk of Corticosteroid-induced Diabetes Mellitus Among the Elderly. Journal of general internal medicine 2002;17(9):717–720. [PubMed: 12220369]
5. van Hooff JP, Christiaans MH, van Duijnhoven EM. Tacrolimus and posttransplant diabetes mellitus in renal transplantation. Transplantation 2005;79(11):1465–1469. [PubMed: 15940032]
6. Molinero LL, Yin D, Lei YM, Chen L, Wang Y, Chong AS et al. High-Fat Diet-Induced Obesity Enhances Allograft Rejection. Transplantation 2016;100(5):1015–1021. doi: 10.10.1097/TP.0000000000001141. [PubMed: 27007226]
7. Quante M, Iske J, Heinbokel T, Desai BN, Cetina Biefer HR, Nian Y et al. Restored TDCA and valine levels imitate the effects of bariatric surgery. eLife 2021;10.
8. Quante M, Iske J, Uehara H, Minami K, Nian Y, Maenosono R et al. Taurodeoxycholic acid and valine reverse obesity-associated augmented alloimmune responses and prolong allograft survival. Am J Transplant 2022;22(2):402–413. [PubMed: 34551205]
9. Hanidziar D, Koulmanda M. Inflammation and the balance of Treg and Th17 cells in transplant rejection and tolerance. Curr Opin Organ Transplant 2010;15(4):411–415. [PubMed: 20613526]
10. Esser N, Legrand-Poels S, Piette J, Scheen AJ, Paquot N. Inflammation as a link between obesity, metabolic syndrome and type 2 diabetes. Diabetes research and clinical practice 2014;105(2):141–150. [PubMed: 24798950]
11. Lei YM, Sepulveda M, Chen L, Wang Y, Pirozzolo I, Theriault B et al. Skin-restricted commensal colonization accelerates skin graft rejection. JCI Insight 2019:In press.
12. Lei YM, Nair L, Alegre ML. The interplay between the intestinal microbiota and the immune system. Clin Res Hepatol Gastroenterol 2015;39(1):9–19. doi: 10.1016/j.clinre.2014.1010.1008. Epub 2014 Nov 1011. [PubMed: 25481240]
13. Pirozzolo I, Sepulveda M, Chen L, Wang Y, Lei YM, Li Z et al. Host-versus-commensal immune responses participate in the rejection of colonized solid organ transplants. J Clin Invest 2022;132(17).
14. McIntosh CM, Chen L, Shaiber A, Eren AM, Alegre ML. Gut microbes contribute to variation in solid organ transplant outcomes in mice. Microbiome 2018;6(1):96. doi: 10.1186/s40168-40018-40474-40168. [PubMed: 29793539]
15. Gurung M, Li Z, You H, Rodrigues R, Jump DB, Morgun A et al. Role of gut microbiota in type 2 diabetes pathophysiology. EBioMedicine 2020;51:102590. [PubMed: 31901868]
16. Li Z, Gurung M, Rodrigues RR, Padiadpu J, Newman NK, Manes NP et al. Microbiota and adipocyte mitochondrial damage in type 2 diabetes are linked by Mmp12+ macrophages. J Exp Med 2022;219(7).
17. Foley KP, Zlitni S, Duggan BM, Barra NG, Anhê FF, Cavallari JF et al. Gut microbiota impairs insulin clearance in obese mice. Molecular metabolism 2020;42:101067. [PubMed: 32860984]
18. Bäckhed F, Manchester JK, Semenkovich CF, Gordon JI. Mechanisms underlying the resistance to diet-induced obesity in germ-free mice. Proc Natl Acad Sci U S A 2007;104(3):979–984. [PubMed: 17210919]
19. Shen H, Goldstein DR. IL-6 and TNF-alpha synergistically inhibit allograft acceptance. J Am Soc Nephrol 2009;20(5):1032–1040. [PubMed: 19357252]
20. Gómez-Hernández A, Otero YF, de las Heras N, Escribano O, Cachofeiro V, Lahera V et al. Brown fat lipoatrophy and increased visceral adiposity through a concerted adipocytokines overexpression induces vascular insulin resistance and dysfunction. Endocrinology 2012;153(3):1242–1255. [PubMed: 22253415]
21. Li Z, Rasic M, Kwan M, Sepulveda M, McIntosh C, Shastry V et al. Oral administration of the commensal Alistipes onderdonkii prolongs allograft survival. Am J Transplant 2023;23(2):272–277. [PubMed: 36804134]

22. Li Z, Rasic M, Kwan M, Sepulveda M, McIntosh CM, Shastry V et al. Oral administration of the commensal Alistipes onderdonkii prolongs allograft survival. American Journal of Transplantation 2023;1. [PubMed: 36695610]
23. Hotamisligil GS. Mechanisms of TNF-alpha-induced insulin resistance. Experimental and clinical endocrinology & diabetes : official journal, German Society of Endocrinology [and] German Diabetes Association 1999;107(2):119–125.
24. Gong T, Liu L, Jiang W, Zhou R. DAMP-sensing receptors in sterile inflammation and inflammatory diseases. Nat Rev Immunol 2020;20(2):95–112. [PubMed: 31558839]
25. Malesza IJ, Malesza M, Walkowiak J, Mussin N, Walkowiak D, Aringazina R et al. High-Fat, Western-Style Diet, Systemic Inflammation, and Gut Microbiota: A Narrative Review. Cells 2021;10(11).
26. Moretti CH, Schiffer TA, Li X, Weitzberg E, Carlström M, Lundberg JO. Germ-free mice are not protected against diet-induced obesity and metabolic dysfunction. Acta physiologica (Oxford, England) 2021;231(3):e13581. [PubMed: 33222397]
27. Logan IE, Bobe G, Miranda CL, Vasquez-Perez S, Choi J, Lowry MB et al. Germ-Free Swiss Webster Mice on a High-Fat Diet Develop Obesity, Hyperglycemia, and Dyslipidemia. Microorganisms 2020;8(4).
28. Peluso I, Palmery M. The relationship between body weight and inflammation: Lesson from anti-TNF-α antibody therapy. Human immunology 2016;77(1):47–53. [PubMed: 26472017]
29. Nurk S, Meleshko D, Korobeynikov A, Pevzner PA. metaSPAdes: a new versatile metagenomic assembler. Genome Res 2017;27(5):824–834. [PubMed: 28298430]
30. Kang DD, Li F, Kirton E, Thomas A, Egan R, An H et al. MetaBAT 2: an adaptive binning algorithm for robust and efficient genome reconstruction from metagenome assemblies. PeerJ 2019;7:e7359. [PubMed: 31388474]
31. Parks DH, Imelfort M, Skennerton CT, Hugenholtz P, Tyson GW. CheckM: assessing the quality of microbial genomes recovered from isolates, single cells, and metagenomes. Genome Res 2015;25(7):1043–1055. [PubMed: 25977477]
32. Chaumeil PA, Mussig AJ, Hugenholtz P, Parks DH. GTDB-Tk v2: memory friendly classification with the genome taxonomy database. Bioinformatics 2022;38(23):5315–5316. [PubMed: 36218463]
33. Parks DH, Chuvochina M, Rinke C, Mussig AJ, Chaumeil PA, Hugenholtz P. GTDB: an ongoing census of bacterial and archaeal diversity through a phylogenetically consistent, rank normalized and complete genome-based taxonomy. Nucleic Acids Res 2022;50(D1):D785–d794. [PubMed: 34520557]
34. Kellersmann R, Zhong R. Surgical technique for skin transplantation in mice. In. Organtransplantation in Rats and Mice: Springer, 1998: 151–154.

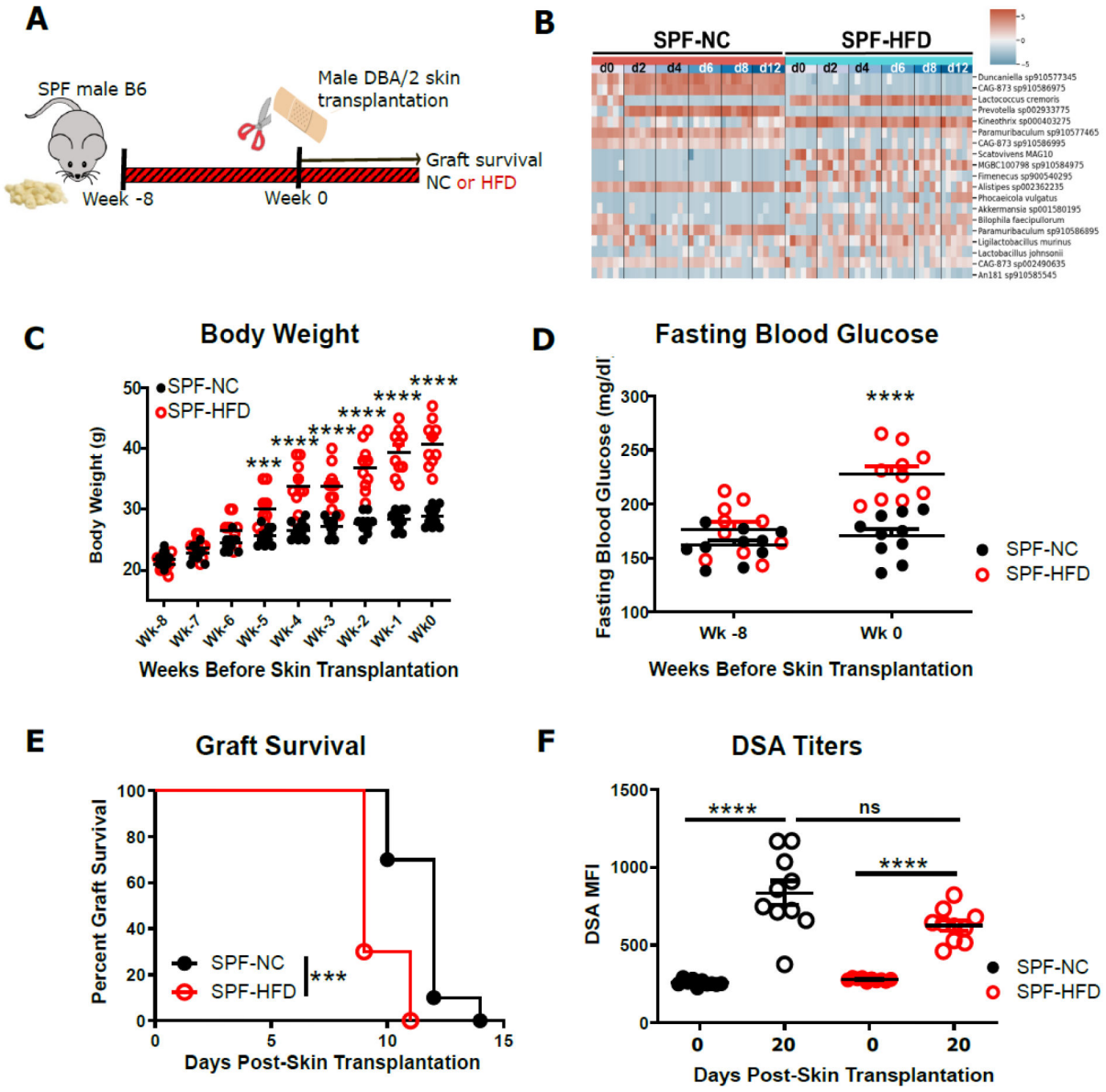

Figure 1. HFD accelerated skin graft rejection and impaired glucose tolerance.

SPF C57Bl/6 (B6, H-2^b) mice were fed either HFD or NC for 8 weeks, then received fully mismatched DBA/2 (H-2^d) skin grafts while continuing with their respective diet. **A.** flow chart depicting the experimental design. **B.** Shotgun sequencing analysis from fecal samples collected longitudinally every 2–4 days (n=6 mice/group) starting after 7 weeks of the respective diets (d0-d12) and prior to skin transplantation. Differentially abundant species in lean versus obese mice are represented. **C.** Weekly changes in body weight of SPF mice on a HFD or NC before skin transplantation. **D.** Fasting blood glucose of SPF mice before and after 8 weeks of HFD or NC. **E.** Allograft survival curves (log-rank test). **F.** Donor specific antibody titers in the serum of recipient mice before and at d20 post-transplantation. (*p<0.05, **p<0.01, ***p<0.001, ****p<0.0001, n=10).

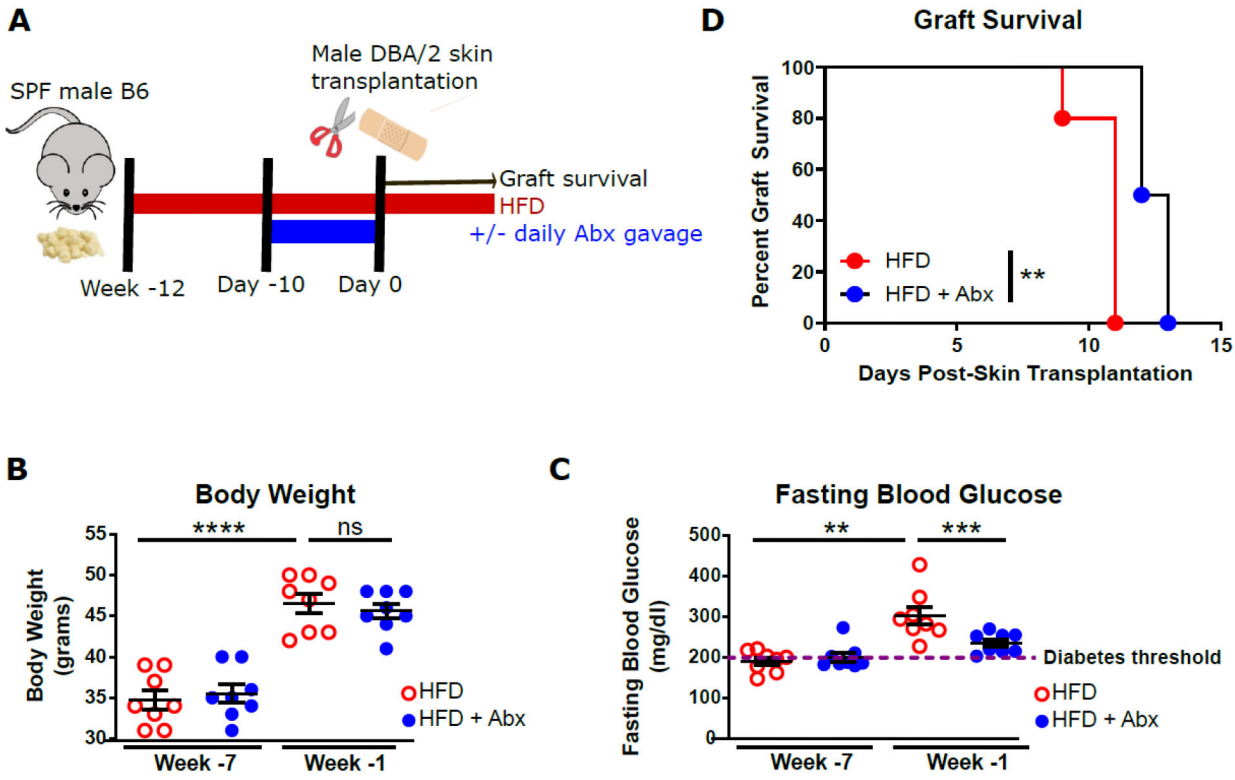

Figure 2. Abx cocktail pre-treatment prolongs skin graft survival and improves glucose tolerance in obese mice.

SPF B6 mice on a HFD were gavaged with a broad-spectrum Abx cocktail Abx or vehicle daily for 10 days prior to transplantation with DBA/2 skin grafts. **A.** flow chart depicting experimental design. **B.** Body weight of HFD-fed mice before and after Abx treatment (n=8). **C.** fasting blood glucose of HFD-fed mice before and after Abx treatment (n=8). **D.** Allograft survival curves (log-rank test, n=4–5). (**p<0.01, ***p<0.001, ****p<0.0001, ns, not significant).

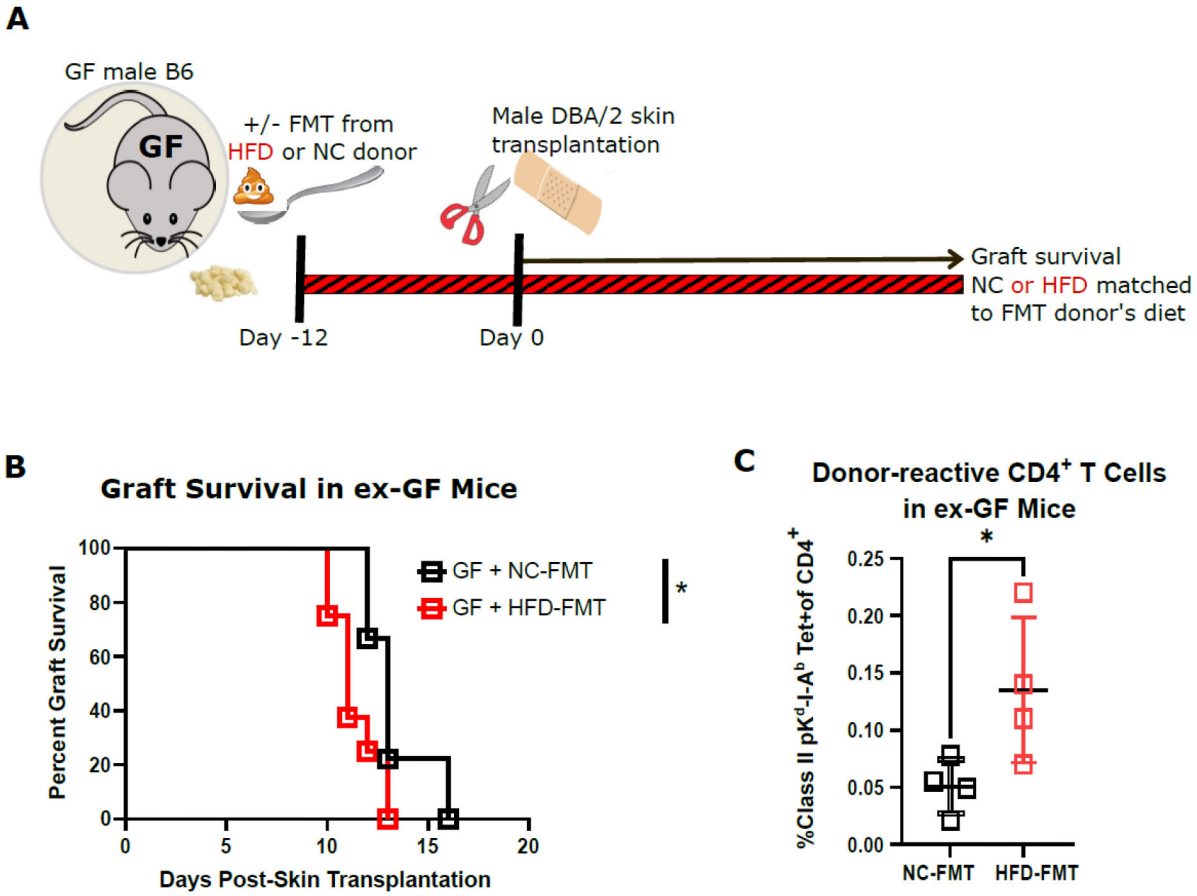

Figure 3. FMT from HFD-fed mice accelerated skin graft rejection in ex-GF mice.

GF male B6 mice received FMT from either HFD-fed or NC-fed SPF mice and started on a HFD or NC diet matched to that of their FMT donors 12 days before they received fully mismatched DBA/2 skin grafts. **A.** flow chart depicting experimental design. **B.** Allograft survival curves (n=8–9, log-rank test). **C.** Proportion of donor-reactive cells among $CD4^+$ T cells in the spleen of ex-GF mice at 3 weeks post-transplantation measured by I-Ab tetramers loaded with a K^d-derived peptide (n=4). (Tet, tetramer, *$p<0.05$).

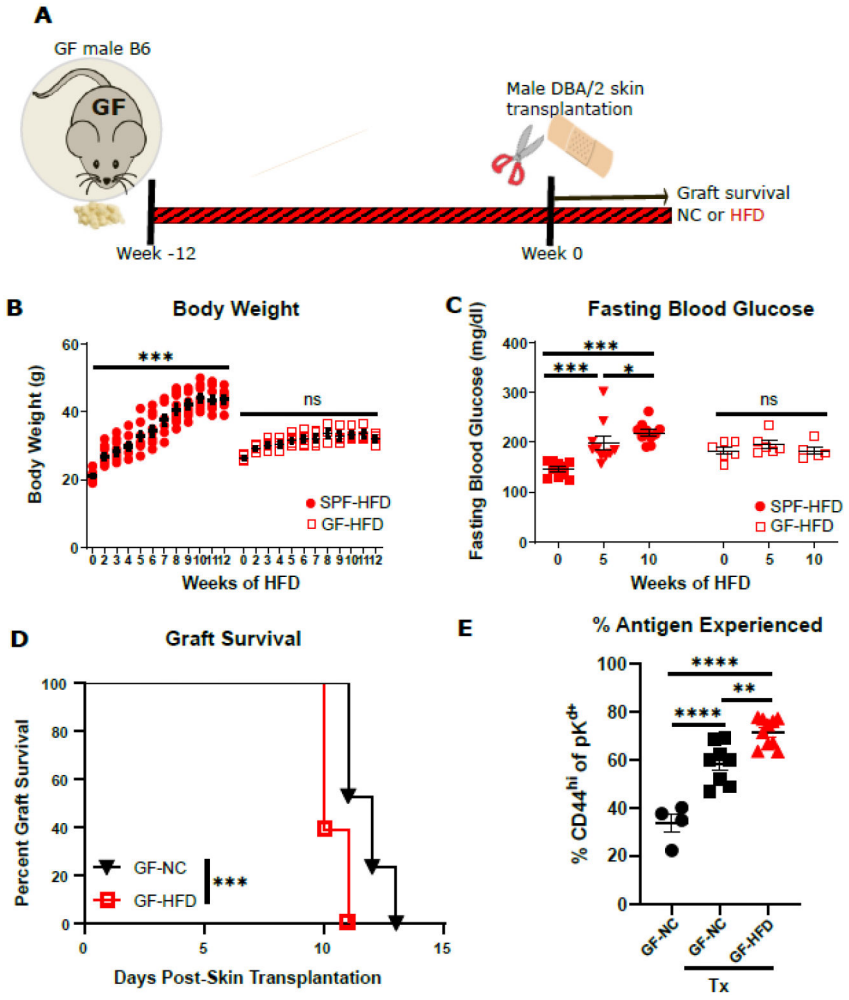

Figure 4. HFD accelerated rejection in GF mice but did not impair glucose tolerance.

GF B6 mice on a HFD or NC for 12 weeks received DBA/2 skin transplants while continuing with their respective diet. **A.** Flow chart of experimental design. **B.** Weekly body weight change of SPF and GF mice on a HFD (n=6–10). **C.** Fasting blood glucose of SPF and GF mice on a HFD (n=6–10). **D.** Survival curves of DBA/2 skin graft in GF mice on a NC or HFD (n=17–18). **E.** Proportion of antigen experienced (CD44hi) cells among all donor-reactive $CD4^+$ T cells in the spleen of GF mice. (*p<0.05, **p<0.01, ***p<0.001, ****p<0.0001, ns, not significant).

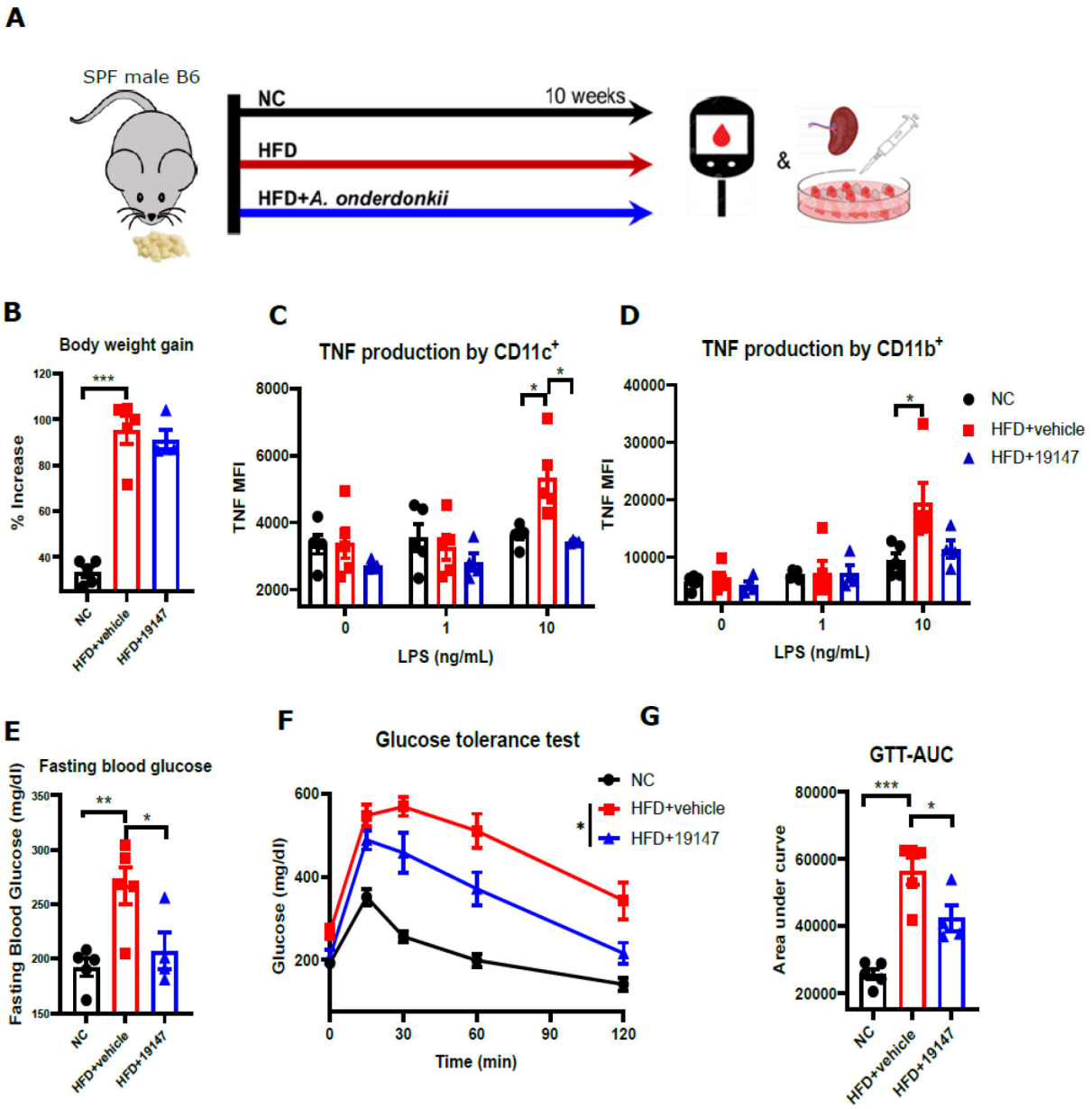

Figure 5. *A. onderdonkii* reduced HFD-induced inflammation and improved glucose tolerance.

SPF male mice were fed a HFD or NC for 10 weeks. One group of HFD-fed mice received *A. onderdonkii* treatment. **A.** Flow chart of experimental design. **B.** Body weight gain of mice after 10 weeks of diet and treatment (percentage increase of body weight at end of experiment relative to initial body weight). **C-F.** Mean fluorescence intensity of tumor necrosis factor by different cell types isolated from the spleen of mice after LPS stimulation in vitro. **G.** Tail blood fasting glucose levels measured by glucometer after 10 weeks of diet and treatment. **H-I.** Intraperitoneal glucose tolerance test after 10 weeks of diet and treatment. GTT-AUC, glucose tolerance test-area under curve, n=4–5, *p<0.05, **p<0.01, ***p<0.001, ****p<0.0001, one-tail p-value, Mean±SEM.